

## The Crilin Calorimeter: an alternative solution for the Muon Collider barrel

S. Ceravolo,<sup>a</sup> F. Colao,<sup>b</sup> C. Curatolo,<sup>c</sup> E. Di Meco,<sup>a,d</sup> E. Diociaiuti,<sup>a,\*</sup> D. Lucchesi,<sup>e</sup> D. Paesani,<sup>a,f</sup> N. Pastrone,<sup>g</sup> G. Pezzullo,<sup>h</sup> I. Sarra,<sup>a</sup> A. Saputi,<sup>i</sup> L. Sestini<sup>e</sup> and D. Tagnani<sup>j</sup>

<sup>a</sup>Laboratori Nazionali di Frascati, Via Enrico Fermi 54, 00044, Frascati, Italy

<sup>b</sup>Enea Frascati, Via Enrico Fermi 45, 00044 Frascati, Italy

<sup>c</sup>INFN, Sezione di Milano, Via Celoria 16, 20133 Milano, Italy

<sup>d</sup>Dipartimento di Fisica, Università degli Studi La Sapienza, Piazzale Aldo Moro 5, 00185, Rome, Italy

<sup>e</sup>INFN, Sezione di Padova, Via Francesco Marzolo 8, 35131 Padova, Italy

<sup>f</sup>Dipartimento di Fisica, Università degli Studi di Tor Vergata, Via della Ricerca Scientifica 1, 00133, Roma, Italy

<sup>g</sup>INFN, Sezione di Torino, Via Pietro Giuria 1, 10125 Torino, Italy

<sup>h</sup>Yale University, New Heaven (CT), USA

<sup>i</sup>INFN, Sezione di Ferrara, Via Saragat 11, 44122 Ferrara, Italy

<sup>j</sup>INFN, Sezione di Roma Tre, Via della Vasca Navale 84, 00146 Roma, Italy

E-mail: [eleonora.diociaiuti@lnf.infn.it](mailto:eleonora.diociaiuti@lnf.infn.it)

The Crilin (CRystal calorImeter with Longitudinal INformation) calorimeter is a semi-homogeneous calorimeter based on Lead Fluoride (PbF<sub>2</sub>) crystals readout by surface-mount UV-extended Silicon Photomultipliers (SiPMs). It is a proposed solution for the electromagnetic calorimeter of the Muon Collider. The calorimeter should operate in a very harsh radiation environment, withstanding yearly a neutron flux of  $10^{14} \text{ n}_{1\text{MeV}} / \text{cm}^2$  and a dose of 100 krad. The proposed Crilin calorimeter is characterized by a modular architecture based on stackable submodules composed of matrices of PbF<sub>2</sub> crystals, with each crystal readout by 2 series of UV-extended SiPMs. To evaluate the effect of this high radiation environment on the PbF<sub>2</sub> crystal, two crystals have been irradiated both with photons and neutrons to study the changes in their transmittance. The results of an intense R&D study to improve the performance of the electronics will be also described

41st International Conference on High Energy physics - ICHEP2022  
6-13 July, 2022  
Bologna, Italy

---

\*Speaker

## 1. Motivation

Muon Colliders (MC) represent a very interesting opportunity as a future accelerator facility allowing to access the energy frontier of the High Energy Physics [1].

Despite the unique advantages, especially in the TeV range, with respect to other accelerating facilities, the decay products of the muons circulating inside of the collider and interacting with the machine elements will create a very harsh radiation environment: two muon beams, each with  $2 \times 10^{12}$  muons per bunch with 750 GeV energy would generate  $4 \times 10^5$  decays/m, leading to  $\mathcal{O}(10^{10})$  background particles reaching the interaction region and entering the detector: the so called Beam Induced Background (BIB).

The actual design for the electromagnetic calorimeter is based on 40 layers of Tungsten absorbers alternated with Silicon pad sensors for a total of 64 million channels in the barrel, thus representing significant technological issue as well as a very expensive solution. Our proposed design, the Crilin calorimeter, is a semi-homogeneous calorimeter based on Lead Fluoride ( $\text{PbF}_2$ ) Cherenkov Crystals [2] readout by surface-mount UV-extended Silicon Photomultipliers (SiPMs).

## 2. The Crilin calorimeter

Crilin has a modular architecture based on stackable and interchangeable sub-modules made of matrices of  $10 \times 10 \times 40 \text{ mm}^3$  Lead Fluoride ( $\text{PbF}_2$ ) crystals each read out by two series of two UV-extended  $10 \mu\text{m}$  pixel SiPMs with a surface of  $3 \times 3 \text{ mm}^2$ .

This proposed configuration allows to obtain: (i) high response speed, due to the Cherenkov nature of the light emitted by the  $\text{PbF}_2$  crystal; (ii) a reduced signal width ensuring an excellent ability to resolve temporally-close events at high rates; (iii) a sufficiently good light collection of  $\sim 1 \text{ p.e./MeV}$ ; (iv) good resistance to radiation as showed in Section 3; (v) fine granularity and scalable SiPMs dimensions.

In order to evaluate the performance of this kind of calorimeter, the W-Si calorimeter was substituted with the Crilin calorimeter in the simulation frame of the Muon Collider.

The implementation is done with the DD4HEP interface to Geant4. The Crilin ECAL barrel design for the Muon Collider consists of five layers with 40 mm thick, and  $10 \times 10 \text{ mm}^2$  of cell area with a dodecahedral geometry. The performance of the two detectors was compared evaluating the jet

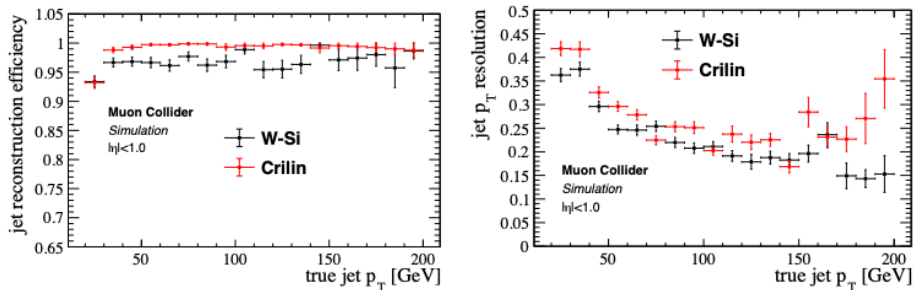


**Figure 1:** Jet reconstruction efficiency (left) and jet  $p_T$  resolution(right) as a function of the jet  $p_T$ , obtained by using the Crilin ECAL barrel (red dots) and the W-Si ECAL barrel (black dots).

reconstruction efficiency and jet  $p_T$  resolutions as they are objects of primary interest for Muon Collider physics. The results are presented in Figure 1. It can be noticed that the performance is similar in the two cases, but a small degradation is observed above true  $p_T$  greater than 170 GeV, because of the Crilin resolution degradation due to the lower number of radiation lengths ( $\sim 19 X_0$ ) compared to the ones of the W-Si ( $\sim 22 X_0$ ).

### 3. Radiation hardness of Crilin components

#### 3.1 PbF<sub>2</sub> crystals

In order to characterize the radiation environment due to the BIB, the latter has been simulated assuming 200 days of operation at  $\sqrt{s} = 1.5$  TeV with Fluka [3] employing a simplified detector geometry.

Figure 2 reports the 1 MeV neutron equivalent fluence and the Total Ionizing Dose (TID) in the detector region, shown as a function of position along the beam axis  $z$  and the radial distance  $r$  from the beam axis.

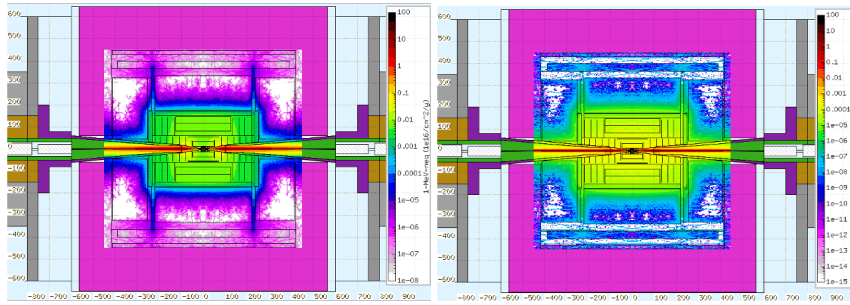


**Figure 2:** 1-MeV-neq fluence (left) and TID (right) in the detector region for a Muon Collider operating at  $\sqrt{s} = 1.5$  TeV.

The expected neutron fluence and dose on the electromagnetic calorimeter region are respectively  $10^{14}$   $n_{1MeV}/(cm^2 \text{ year})$  and  $10^{-4}$  Grad/year.

The radiation hardness of the crystals was checked both for TID and NIEL at the Calliope Facility of Enea Casaccia with  $^{60}\text{Co}$  [4] and at the Frascati Neutron Generator Facility (FNG) of Enea Frascati with 14 MeV neutrons [5] using two PbF<sub>2</sub> crystals, one without wrapping, dubbed “naked”, and one with Mylar wrapping. The results of these irradiation are reported in Figure 3. For what concerns the photon irradiation, the maximum degradation observed is at the level of  $\sim 40\%$ , in between of the degradation observed in [6] and [7]. The transmittance spectrum after the neutron irradiation was evaluated 14 days after the exposure. No alteration in the transmittance spectrum is observed.

#### 3.2 Silicon Photomultipliers

The present SiPMs choice for the Crilin calorimeter is Hamamatsu S14160-3015PS SMD sensors [8]. The  $15 \mu\text{m}$  SiPM pixel-size were selected for high-speed response, short pulse width and to better cope with the expected total non-ionising dose (TNID). Since the granularity of the

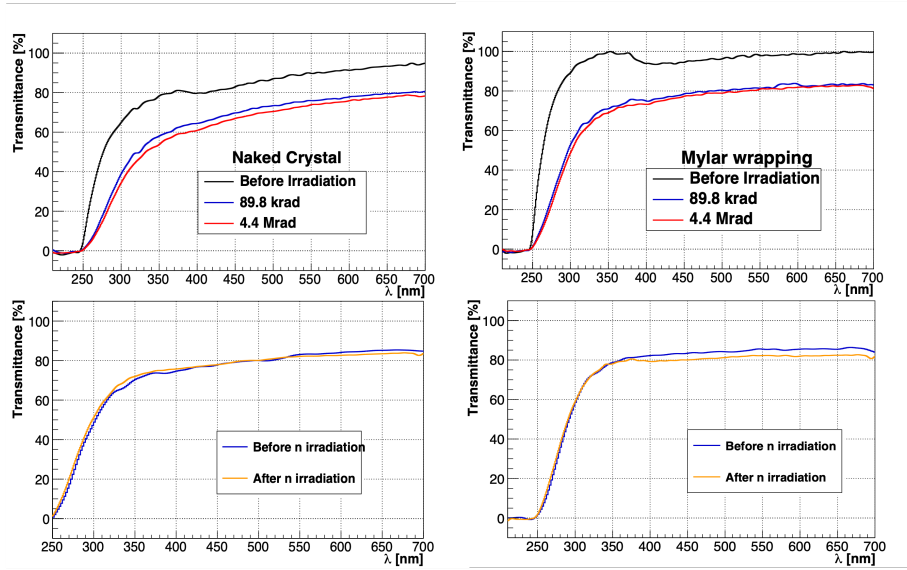


**Figure 3:** Top: Transmission spectra obtained in the different irradiation steps for the naked crystal (left) and the crystal with Mylar wrapping (right). Bottom: Transmission spectra obtained before and after the neutron irradiation for the naked crystal (left) and the crystal with Mylar wrapping (right)

calorimeter scales with the pixel dimensions it is also under investigation the possibility to use 10  $\mu\text{m}$  pixel-size SiPMs. Two 15  $\mu\text{m}$  and two 10  $\mu\text{m}$  pixel-size SiPMs have been exposed at FNG for 80 hours to a neutron flux up to  $10^{14}$  n/cm<sup>2</sup>. After the irradiation, the SiPMs I-V curves were measured at different temperatures ranging from -10 °C to 0 °C. In Figure 4 the leakage currents of the two different pixel-sized SiPMs after the irradiation as a function of the bias voltage,  $V_{bias}$ , are reported.

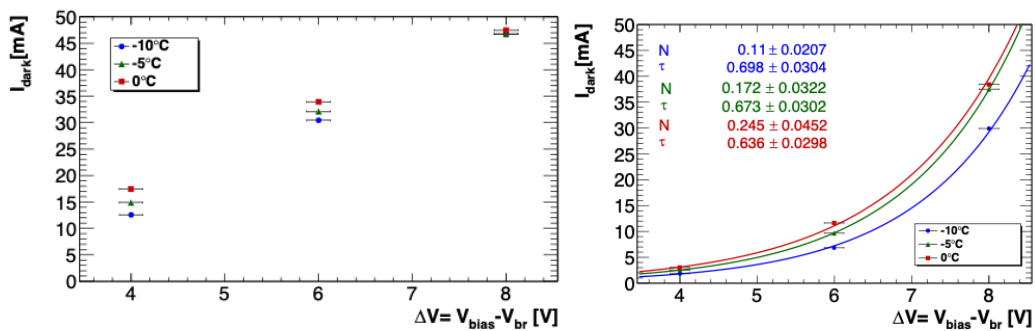


**Figure 4:** 15  $\mu\text{m}$  pixel (left) and 10  $\mu\text{m}$  pixel (right) SiPM breakdown voltage as a function of the operating temperature.

Clearly, to cope with the harsh environment expected for the Muon Collider, the better SiPM choice would be the 10  $\mu\text{m}$  pixel-size.

#### 4. Time resolution performances

A preliminary study of timing performance reachable with the developed Front-End Electronics (FEE) was carried out with two 15  $\mu\text{m}$  pixel SiPM connected to a prototype version of the FEE and illuminated with a picosecond UV laser source by Hamamatsu.

The waveform of the signal present a considerably sharp pulse with a  $\sim 2$  ns rise time and a  $\sim 70$  ns full width. The timing reconstruction was performed using Constant Fraction method ( $\sim 30\%$  of peak amplitude) on a LogNormal fit.

Different configurations were tested: (a) Constant 1 V laser pulse amplitude and fixed 40 Gps sample rate, while laser repetition rate was increased from 50 kHz up to 5 MHz in 5 steps. (b) Fixed laser amplitude and fixed 100 kHz laser repetition rate, while the oscilloscope sampling rate was swept in the range 2.5 to 40 Gps. (c) Fixed laser repetition rate and sampling frequency, while the laser amplitude was swept over the FEE dynamic range in 6 steps.

Results of these three configurations are reported in Figure 5.

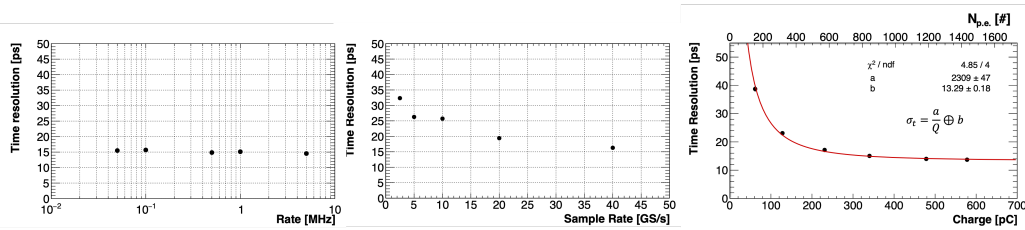


**Figure 5:** Left: Time resolution as function of the laser repetition rate. Center: Time resolution as function of sample rate. Right: Time resolution as a function of the collected charge.

A constant behaviour with respect to the laser repetition rate is observed, meaning that the waveform remains unchanged in the 50 kHz-5MHz range. On the other hand, a strong dependence on the sample rate is seen: e.g. the time resolution at 2.5 GS/s is twice the one at 40 GS/s.

In Figure 5 (Right) the time resolution as a function of the mean value obtained from a gaussian fit to the collected charge is reported; a resulting 13 ps constant term (b) contribution to timing resolution was evaluated on data fitted with  $\sigma_t = \frac{a}{Q} \oplus b$ . The number of collected photoelectrons was evaluated as  $N_{p.e.} = \frac{\mu Q}{G_{FEE} \times G_{SiPM} \times e}$ , where  $G_{FEE} = 7$ ,  $G_{SiPM} = 3.6 \times 10^5$  and  $e$  is electron charge.

#### 5. The Crilin prototypes

A first prototype of the Crilin calorimeter (see Figure 6), Proto-0, made of a single layer of 2 crystals and read out by 4 SiPMs was built in 2021. It was tested at the Beam Test Facility of the LNF with 500 MeV electrons in July 2021 and at the H2 test facility of CERN with 120 GeV electrons in August 2021 [9] obtaining promising results: a timing resolution less than 100 ps for deposited energies greater than 1 GeV, and  $\sim 1$  p.e./MeV of light yield.

At this point of the R&D it is pivotal to validate the design choices both in terms of mechanics, cluster reconstruction and shower profile. For this reason a new prototype is going to be realized. After a simulation optimization, Crilin dimensions have been increased to  $8.5 X_0$  ( $\sim 0.3 \lambda$ ), a good compromise between an acceptable containment of 100 GeV electrons and costs. Proto-1 will have

two layers of  $3 \times 3$  PbF<sub>2</sub> crystals, each readout with  $10 \mu\text{m}$  UV-extended SiPMs. The operational temperature will be  $0/-10 \text{ }^\circ\text{C}$  and the performance will be validated in a dedicated test beam.

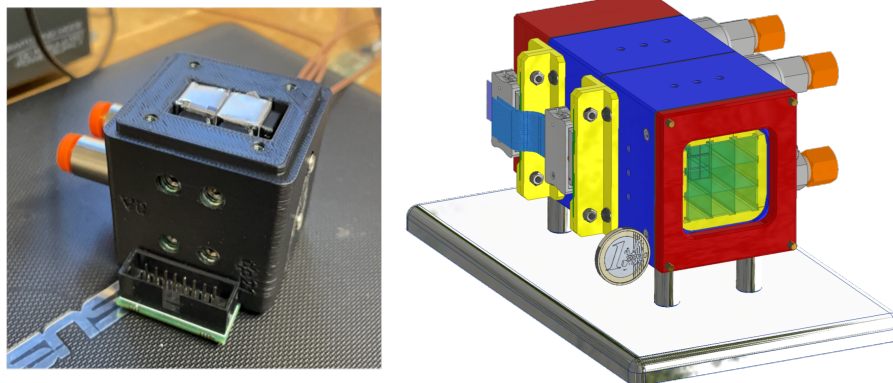


**Figure 6:** Left: picture of Proto-0. Right: CAD 3D model of Proto-1.

## 6. Conclusion

Crilin is a semi-homogeneous calorimeter with longitudinal segmentation and excellent timing resolution. It represents a good compromise between homogeneous and sampling calorimeter and is well quoted as alternative solution to W-Si ECAL for future Muon Colliders. Before the construction of the Proto-1, several tests on single components have been performed: irradiation studies both with neutrons and photons on PbF<sub>2</sub> crystals indicated no significant damages up to 80 krad TID and  $10^{13} \text{ n/cm}^2$  fluence; neutron irradiation up to  $10^{14} \text{ n/cm}^2$  on SiPMs showed the necessity to use  $10 \mu\text{m}$  SiPMs. Proto-1 is going to be assembled by the end of 2022 and it will be fundamental to validate the technical choices made.

## References

- [1] Long, Kenneth R., et al. "Muon colliders to expand frontiers of particle physics." *Nature Physics* 17.3 (2021): 289-292.
- [2] Anderson, D. F., et al. "Lead fluoride: An ultra-compact Cherenkov radiator for EM calorimetry." *Nuclear Instruments and Methods in Physics Research Section A: Accelerators, Spectrometers, Detectors and Associated Equipment* 290.2-3 (1990): 385-389.
- [3] A. Ferrari et al., "FLUKA: a multi-particle transport code", CERN-2005-10 (2005), INFN/TC\_05/11, SLAC-R-773.
- [4] Calliope Brochure, <https://www.enea.it/it/seguici/pubblicazioni/pdf-opuscoli/calliope.pdf>
- [5] FNG website, <http://www.fusione.enea.it/LABORATORIES/Tec/FNG.html.it>

- [6] G.H. Ren et al., "Optical Absorption on Cubic  $\beta$ -PbF<sub>2</sub> Crystals." Chinese Physics Letters 18.7 (2001): 976-978.
- [7] P. Achenbach et al., "Radiation resistance and optical properties of lead fluoride Cherenkov crystals." Nuclear Instruments and Methods in Physics Research Section A: Accelerators, Spectrometers, Detectors and Associated Equipment 416.2-3 (1998): 357-363.
- [8] Hamamatsu S14160-3015PS datasheet, [https://www.hamamatsu.com/content/dam/hamamatsu-photonics/sites/documents/99\\_SALES\\_LIBRARY/ssd/s14160-1310ps\\_etc\\_kapd1070e.pdf](https://www.hamamatsu.com/content/dam/hamamatsu-photonics/sites/documents/99_SALES_LIBRARY/ssd/s14160-1310ps_etc_kapd1070e.pdf)
- [9] AIDAinnova 1st Annual Meeting, [https://indico.cern.ch/event/1104064/contributions/4801240/attachments/2417197/4136687/Moulson\\_220329WP8.pdf](https://indico.cern.ch/event/1104064/contributions/4801240/attachments/2417197/4136687/Moulson_220329WP8.pdf)